京 都 大 学 防 災 研 究 所 年 報　第48号 C　平成17年4月
Annuals of Disas. Prev. Res. Inst., Kyoto Univ., No. 48 C, 2005

Analysis and Prediction of Anomalous Weather and Atmospheric Hazards

Hiromasa KAWAI, Tatsuya IWASHIMA, Hiromasa UEDA,
Takashi MARUYAMA, Hirohiko ISHIKAWA, Hitoshi MUKOUGAWA,
Mitsuaki HORIGUCHI, Takao IGUCHI and Tokihiko ARAKI

Synopsis

This paper describes the analysis of various phenomena related with anomalous weather and its hazards, which consists of three parts. Predictability and a possible tropospheric precursor of a zonal-wavenumber (WN) 1 stratospheric sudden warming (SSW) event occurring in December 2001 are examined in the first part, using all ensemble members of the 1-month forecasts carried out by the Japan Meteorological Agency (JMA). The second part shows the field investigation on the severe damages of structures including Itsukushima Shrine, a designated world heritage site on Miyajima Island in the prefecture of Hiroshima, Japan, induced by the typhoon 0418 which attacked on September 7, 2004. The last part show the results of several analyses, which were carried out to investigate abnormal typhoons hit Japanese territory in 2004. The seasonal march of the sea surface temperature (SST) were investigate and reproduce the meteorological situation by using a mesoscale numerical model. The Asian monsoon is also investigate to understand the abnormal weather in summer

Keywords: anomalous weather, stratospheric sudden warming, Arctic Oscillation (AO) signature, Typhoon 0418, wind induced damage, Itsukushima shrine, sea surface temperature, GMS-5, PSU/NCAR MM5, Asian monsoon

1. Predictability of a Sudden Warming Event occurring in December 2001

1.1 Introduction

Stratospheric sudden warmings (SSWs) are the most spectacular planetary-scale event in the wintertime stratospheric circulation. The basic mechanism of the SSW has been already established by Matsuno(1971) in the framework of dynamical interactions between stratospheric zonal flows and upward propagating planetary waves from the troposphere. However, tropospheric precursors which promote the upward propagation of planetary waves for the onset of the SSW have not been fully documented. Recently, the downward influence of the stratospheric circulation change on the troposphere has been a central issue of the stratosphere-troposphere dynamical interaction inspired by the work of Baldwin and Dunkerton (1999). They statistically showed evidence of downward propagation of Arctic Oscillation (AO) signature from 10 hPa level to surface on a time-scale of about 3 weeks. Since the occurrence of SSW well corresponds to a large negative deviation in the AO signature time series in association with weak polar vortex, their results suggest enhancement of meridional meandering of the tropospheric circulation after the warming peak of SSW events. In fact, Baldwin and Dunkerton (1999, 2001) have shown that weak polar vortex events in the stratosphere precede anomalous tropospheric weather regimes with the southward displacement of the storm track from its climatological position. Therefore, in order to improve the forecast skill of anomalous weather in the troposphere, it is necessary to examine the dynamical predictability of SSW events using state-of-the-art numerical weather prediction models.

In this study, by the use of all ensemble members of the Japan Meteorological Agency(JMA) 1-month forecasts including predictions from perturbed initial

conditions, we try to reveal the predictability and the tropospheric precursor of a major SSW event occurring in Dec 2001. The ensemble predictions also enable us to examine the sensitivity of the SSW forecast to the initial condition.

1.2 Data

We used operational ensemble 1-month (34-day) forecast data sets provided by JMA from Nov 2001 to Jan 2002. The JMA ensemble 1-month prediction has been carried out at 1200UTC every Wednesday and Thursday with 12 perturbed and 1 unperturbed initial conditions. Numerical integrations are conducted using a JMA global spectral model (JMA-GSM0103) with triangular 106 truncation (T106) and 40 vertical levels up to 0.4 hPa (JMA, 2002). The initial perturbations are obtained using the Breeding of Growing Modes (BGM) method (Toth and Kalnay,1993). They are confined north of 20N with an amplitude set to be 14.5% of the climatological root-mean-square variance at 500-hPa height. The forecast data have been archived every 24 h for the 34-day prediction period on a 2.5 X 2.5-degree longitude-latitude grid at 22 levels from 1000 to 1 hPa. To verify model forecasts, JMA Global Analyses data set with 1.25-degree horizontal resolution at 23 levels from 1000 to 0.4 hPa is used.

1.3 Results

The daily time series of 10-hPa zonal mean temperature Tat 80N (thick solid line in Fig. 1) clearly shows the occurrence of warming event in late December. The temperature attains its peak on 28 Dec 2001. As documented by Naujokat et al. (2002), this warming is classified as a major SSW caused by the amplification of zonal wavenumber (WN) 1 planetary wave. The thin lines in Fig.1 show the predicted T by the JMA ensemble 1-month forecasts. Almost all the members fail to predict the occurrence of this warming event for the forecasts starting from 28 and 29 Nov (Fig. 1a). However, some members successfully reproduce the SSW event for the forecasts starting from 5 and 6 Dec (Fig. 1b). All the ensemble members staring from 12 and 13 Dec also well predict the warming episode (Fig. 1c). Thus, the initial conditions on 12 and 13 Dec are considered to include a necessary precursor for the onset of the SSW.

The long-range predictability of the SSW with a lead time of more than 2 weeks reported by Mukougawa and Hirooka (2004) (hereafter referred to as MH)is also confirmed for this case using the ensemble forecasts. Moreover, it is noteworthy that the spread among ensemble members becomes very large for the forecasts starting from 5 and 6 Dec compared with the forecasts staring from the adjacent weeks. This indicates high sensitivity to the initial condition for the prediction of the SSW during its onset period.

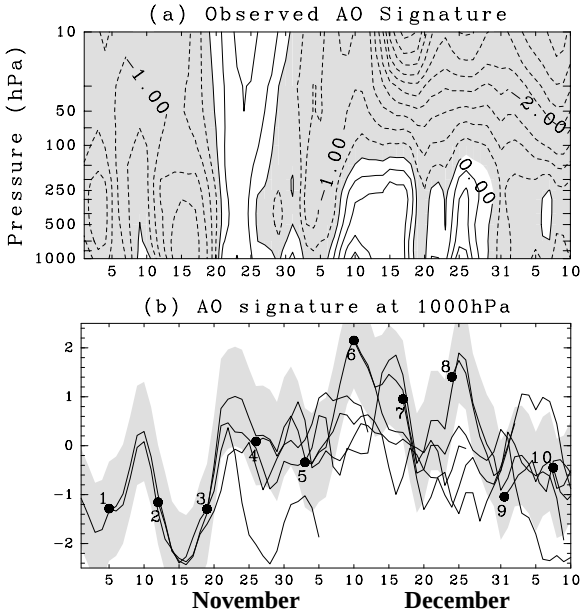

Fig.1 Time variation of 10-hPa T at 80N from 20 Nov 2001 through 20 Jan 2002 for the analysis (thick solid line) and the JMA ensemble forecasts (thin solid lines) starting from 28 and 29 Nov (a), 5 and 6 Dec (b), and 12 and 13 Dec 2001 (c). The broken and dotted lines in (b) denote run A and run B, respectively.

In order to find a necessary precursor for the SSW, we first compare the behavior of the best forecast (run A) and the worst forecast (run B) among ensembles starting from 5 and 6 Dec 2001 in detail. The prediction skill for the SSW is assessed by the 10-hPa T at 80N on 28 Dec, when the observed T attains its peak. These two forecasts start from 6 Dec, and are shown by the broken and dotted lines with labels in Fig. 1b. Since this warming event was caused by the WN 1 amplification, it is reasonable to examine the predicted WN 1 activity to detect a bifurcation point" after which run A and run B differ significantly. By examining the temporal behavior of the vertical component of Eliassen--Palm (E-P) flux of WN 1 (not shown), it is found that the difference between run A and run B became noticeable after around 13 Dec. This period also coincides with the initialization time of

the next ensemble forecasts (Figure 1c), which succeeded in predicting the SSW. Therefore, we focus on the circulation difference between the forecasts around 13 Dec.

The meridional configuration of zonal-mean zonal wind U, which affects the propagation and generation of planetary waves, is a key ingredient for the prediction of SSWs as shown in MH. The left panels in Fig. 2 show 3-day mean U profile below 10 hPa during 12--14 Dec. Striking difference of run B (bottom row) from the observation (top row) and run A (middle row) is found in high latitudes of the troposphere. For run B, weak easterlies exist around 80N with relatively strong westerlies around 60N in the upper troposphere. By contrast, for the observation and run A, a rather strong westerly jet in the upper troposphere is situated around 80N with weak westerlies to the south. The U profile in high latitudes is associated with a prominent blocking high in the Atlantic sector as seen in the right panels in Fig. 2, which show 3-day mean 500-hPa geopotential hight distribution for the same period. The developed blocking high over Great Britain shifts the Atlantic westerly jet poleward in the observation (top row) and run A (middle row). However, in run B (bottom row), the blocking is in a decaying stage by downstream emanation of Rossby wave activity.

In order to check the statistical significance of the relationship between the characteristic U profile and the subsequent occurrence of the SSW revealed by the above comparison, we made an regression analysis using all (26) ensemble members of the JMA 1-month forecasts starting from 5 and 6 Dec. Figure 3a shows the regressed anomaly of the predicted 3-day mean U during 12--14 Dec against the predicted 10-hPa T on 28 Dec, corresponding to the warming peak. Here, the anomaly is defined as the deviation from the ensemble mean of the forecasts (Fig. 3b). From this figure, we confirm that the dipole structure of upper-tropospheric U in high latitudes with positive (negative) anomalies around 80N(60N) is well correlated with the subsequent occurrence of the SSW after about 2 weeks, consistent with the previous analysis on the best and worst predictions. Positive U anomalies found in subtropical regions seem to be less significant in the upper troposphere.

Figure 3a also shows the regressed anomaly of WN 1 E-P flux with statistical significance. Associated with the U anomaly, WN1 activity tends to propagate poleward. Although the upward propagation of the ensemble averaged WN1 activity is most active around 60N in the lower stratosphere (Fig. 3b), the upward propagation is significantly enhanced around 70N corresponding roughly to the node of the U anomaly.

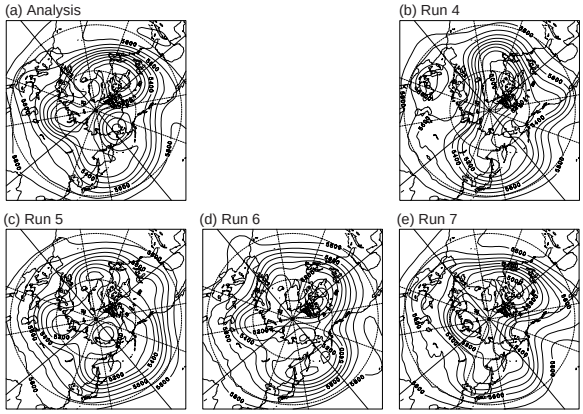

Fig.2 Latitude-height cross sections of U (m/s) (left panels) and 500-hPa geopotential height (right panels) averaged over 12—14 Dec for the analysis (top row), run A (middle row), and run B (bottom row).

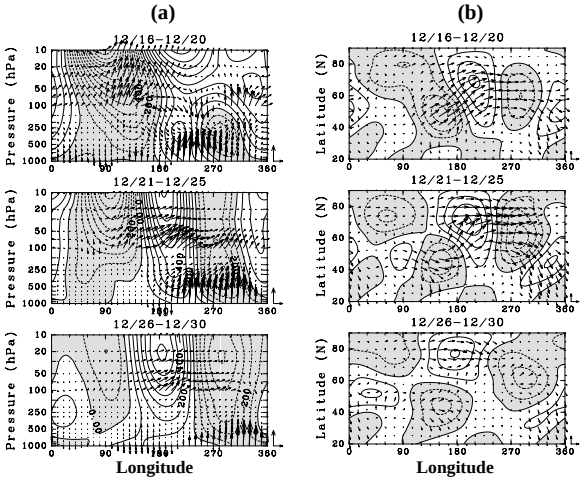

Fig.3 (a) Regressed anomaly of the predicted 3-day mean U during 12--14 Dec upon the predicted 10-hPa T at 80N on 28 Dec using all ensemble forecasts starting from 5 and 6 Dec (m/s). The light (heavy) shades indicate regions where the statistical significance of the anomaly exceeds 90 (95)%. The regressed WN 1 E-P flux anomalies (kg/s^{2}) of which vertical components are significant at the 90% level are also shown. The magnitude of the vector is multiplied by 10. (b) Ensemble average of the predicted 3-day mean U along with the corresponding E-P flux vectors averaged over 12--14 Dec. E-P flux is scaled by the reciprocal square root of the pressure. The magnitude of the reference vectors at 1000 hPa are shown in the lower right corner.

These result suggests that the enhancement of poleward and upward propagation of WN 1 activity in the troposphere and the lower stratosphere associated with the distinctive U anomaly promotes the subsequent upward propagation of the WN 1 activity, which in turn causes the SSW. The refractive properties of the zonal wind anomaly are also in concord with the regressed anomaly of WN1 E-P flux. The refractive index squared (e.g., Andrews et al.,1987) of stationary WN 1 for the regressed zonal wind anomaly shown by Fig. 3.3a has a local maximum around 80N at the tropopause level, which tends to deflect the propagation of WN1 activity poleward and promotes its upward propagation.The meridional curvature of the westerly jet in high latitudes is responsible for the local maximum of the refractive index.

The high sensitivity to the initial condition for the SSW forecast found in Figure 1b could be inferred from Figure 4. This figure shows the direction of the maximum dispersion among all ensemble members, represented by the leading Empirical Orthogonal Function (EOF) of the predicted 3-day mean U for 12--14 Dec of the ensemble forecasts initialized at 5 and 6 Dec. The EOF analysis was made for a domain from 1000 to 1 hPa poleward of 20N, and the data were weighted by the square root of the cosine of latitude as well as the square root of density at each level. The first EOF mode explains 36% of the total variance of U around the ensemble mean. The regressed U anomalies to the first principal component (PC1) have maxima in the upper troposphere, and are characterized by a barotropic tripole structure with nodes around 40N and 65N. These features are very similar to the U profile correlated with the occurrence of the SSW shown in Figure 3a except for a slight equatorward shift by 5-degree. Thus, the coincidence could explain the reason why the high sensitivity to the initial condition is observed during the onset of the SSW. The regressed WN 1 E-P flux anomaly to PC1 as depicted by arrows in Figure 4 also supports this conjecture. The upward propagation in the lower stratosphere around 65N is significantly enhanced as in Figure 3a, which would trigger the SSW.

1.4 Concluding Remarks

By the use of all ensemble members of the 1-month forecasts performed by the JMA, a high sensitivity to the initial condition for the prediction of a SSW event

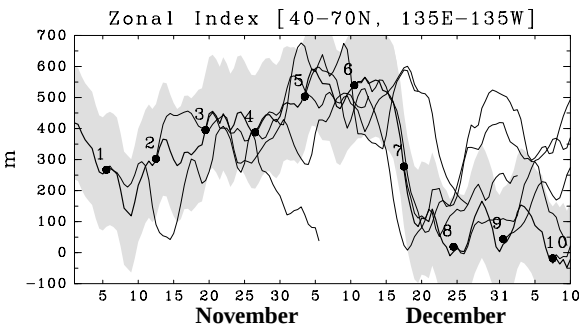

Fig.4 Same as Fig. 3a, but for the regressed U and E-P flux vectors upon PC1 of the predicted 3-day mean U for 12--14 Dec of the ensemble forecasts starting from 5 and 6 Dec (m/s).

occurring in Dec 2001 was detected during its onset period. It was found that a distinct tropospheric U profile, with positive (negative) anomalies around 80N (60N) during this period, is significantly related to the subsequent warming in the stratospheric polar region. This characteristic U anomaly was associated with the blocking over the Atlantic sector, and was also identified as the leading EOF of the U variation among ensemble members. Hence, we can conclude that the high sensitivity to the initial condition for the SSW prediction is owing to the coincidence between these two U anomalies. This is also supported by the fact that the upward propagation of WN 1 activity is enhanced in the lower stratosphere associated with the U anomaly, which triggers the subsequent warming episode.

1.5 Acknowledgments

We would like to thank all the members in Numerical Prediction and Climate Prediction Divisions in JMA for providing us 1-month forecast data sets of JMA.The GFD-DENNOU Library was used for the graphics.

2. Investigation of Damage to Itsukushima Shrine from Typhoon 0418

2.1 Location and Meteorological records

Typhoon 0418 began its approach on the 28th of August and passed by Honshu, the main island of Japan, at a point nearest to the city of Hiroshima during the daytime on September 7, 2004 as shown in figure 5 and 6. Itsukushima Shrine, is a designated world heritage site located on Miyajima Island in Hiroshima bay as shown in Figure 7. The shrine is located at the bottom of an inlet as shown in Figure 8. There are rather high peaks and deep valleys that rise from the southern bank of the inlet. The meteorological records obtained for this study came from Hiroshima Local Meteorological Observatory in downtown Hiroshima city and from the Miyajima fire station near the shrine. The strongest mean wind speeds and the change of wind directions occurred between two

Fig.5. Location of Hiroshima and the path of Typhoon 0418

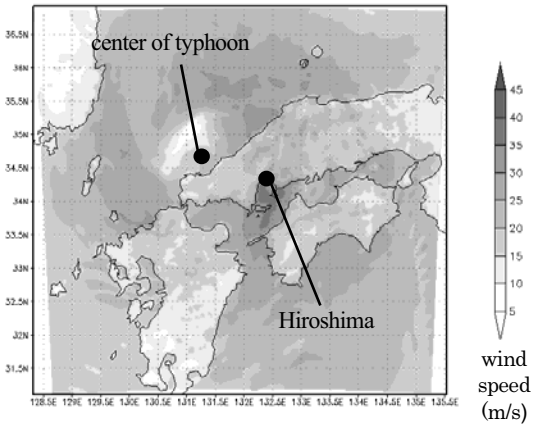

Fig.6. Wind distribution around the center of Typhoon 0418 at 14:00, Sep. 7

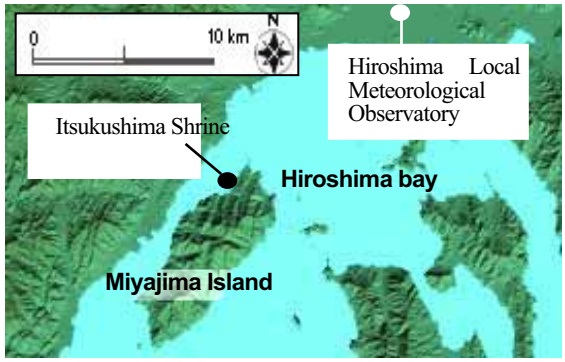

Fig.7 Location of Miyajima Island and Itsukushima Shrine in Hiroshima bay

Fig.8 Bird eye's view of Miyajima Island from north

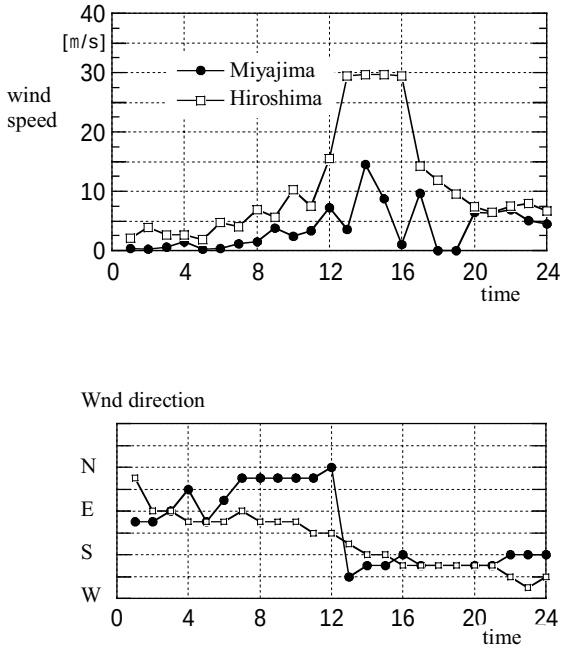

Fig.9 Meteorological records at Hiroshima Local Meteorological Observatory and Miyajima fire station

to four o'clock in the afternoon. The maximum peak gust of 60.2m/s was recorded at 14:20 and is the strongest wind ever measured by Hiroshima Local Meteorological Observatory. A maximum peak gust of 47.6m/s was recorded at 13:25 by the Miyajima fire station.

2.2 Overview of damage in Hiroshima prefecture

According to the damage reports later published by the Hiroshima Prefectural Government, there were 146 people injured in total, including 5 deaths and 23 serious injuries that all resulted from Typhoon 0418.

A total of 17,546 buildings were damaged, including 22 houses that were completely destroyed, 237 houses that were badly damaged, 12,764 houses that were partially damaged, 1,131 houses that were flooded over the floor and 3,392 houses that were flooded under the floor. About 2.88 million people lived in Hiroshima prefecture with the total number of households at about 1.17 million, meaning that 0.005% of its residents and 1.5% of its buildings suffered, respectively. The damage was mainly due to strong winds and the cost of damage was estimated to be about 14 billion yen (roughly 130 million US$).

Various kinds of damage was caused from the strong winds on Miyajima Island as shown in photo 1. We can note the variety of wind directions around Itsukushima Shrine as shown in figure 10 caused by the mesoscale change of wind field and the geographical features of the island.

2.3 Damage to Itsukushima Shrine

The damage to the structures at Itsukushima Shrine was caused by not only the strong winds but also the high tide and waves. The roof tiles of the Noobutai were blown away by the wind and came down along the southern valley as shown in photo 2.①. Hiwada, pieces of cypress bark used for roofing, were torn loose by the wind on the roof of the western corridor of the main building (Honshaharaiden) as shown in photo 2.② and ③. Butai, the wooden float, in front of the main building, was damaged from both the high tide and the waves (photo 2.③). The floors of the corridors that surround and connect to each building were also damaged from the high tide and the waves (photo 2. ④). Sagakubou, a shed for music located on the left-hand side of the main building, was completely destroyed and washed out to sea by the high tide and the waves (photo 2.⑤).

2.4 Conclusion

This paper presents a brief summary of the damage to Itsukushima Shrine caused by Typhoon 0418 in the Prefecture of Hiroshima on September 7th 2004.

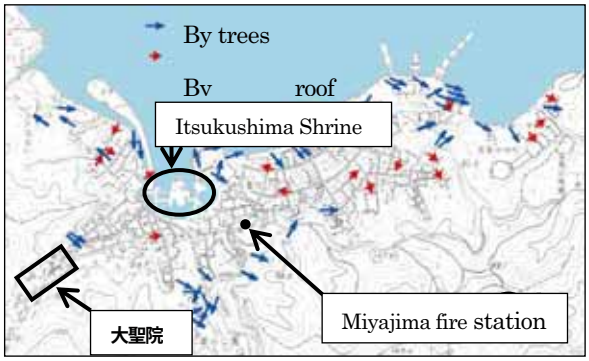

Fig.10 Distribution of wind directions around Itsukushima Shrine estimated by broken trees and the roof damage

a. A collapsed wall

b. Damage to ro

c .Broken trees

Photo 1 Various finds of damage recorded around Itsukusima Shrine in Miyajima Island

① Noobutai

② Western corridor

③ Honshaharaiden and Butai

④ Maroudojinja

⑤ Footings where Ugakubou stood

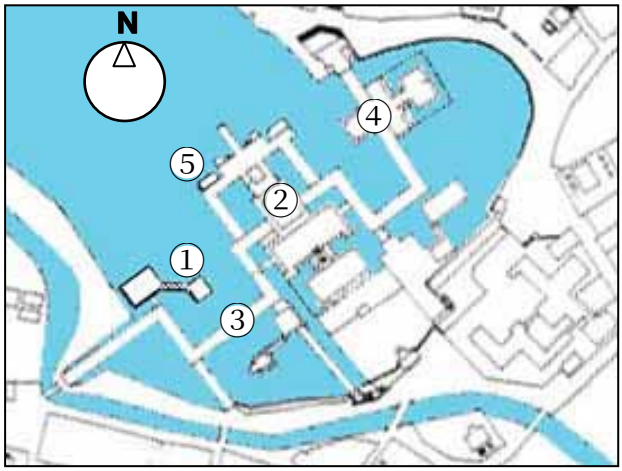

Location

Photo 2　Damage to Itsukushima Shrine

3. Severe storm and the related study

3.1 Typhoons in 2004

Ten typhoons among 29 hit Japan Islands in 2004. This number is the highest record since 1951 (Fig. 11). The number of typhoon genesis, 29, is not abnormal, but it is remarkable that as many as 10 typhoons hit Japanese territory.

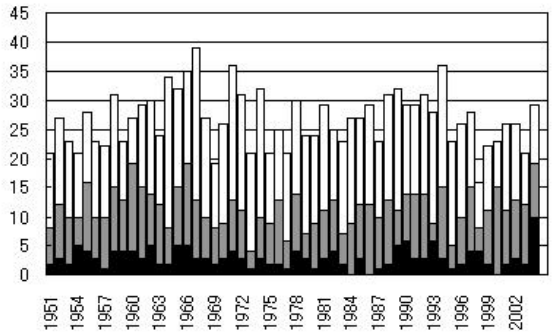

Fig.11 Numbers of typhoon genesis (white), approached to Japanese territory(gray) and hit Japanese territory(black) since 1951.

In order to investigate this, the seasonal march of the sea surface temperature (SST) is examined together with the variation of the Bonin High. Figure 12 shows a comparison of 10 day average of SST and surface pressure in early June of 2002 and 2004. It is seen that the SST is higher and the Bonin High is stronger in 2004. This forms a favorable situation that the typhoons in early summer keep their strength to reach Japan Island.

In order to investigate the typhoon and the associated hazardous condition, a mesoscale numerical model (PSU/NCAR MM5) is used to reproduce the meteorological situation. Figure 13 is a bird eye view of the simulated T0423. The near surface stream line and the distribution of rainwater are shown. It is seen that the precipitating cloud prevails at the northern side of the typhoon center. Figure 14 is the accumulated precipitation associated with the typhoon passage. It also includes the pre-curser precipitation associated with front. The simulated precipitation is in good agreement with observation.

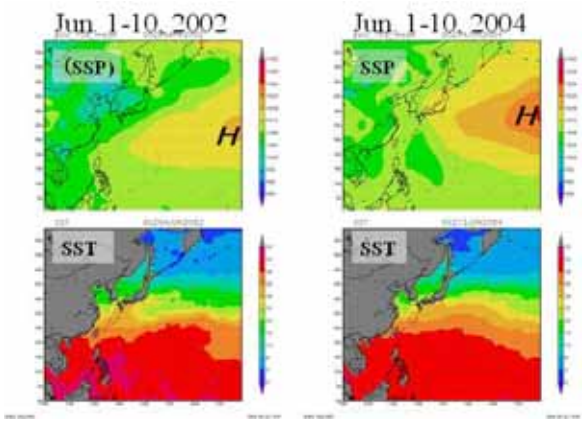

Fig.12 Comparison of Sea Surface Pressure (SSP) and Sea Surface Temperature (SST) of early June of 2002 and 2004.

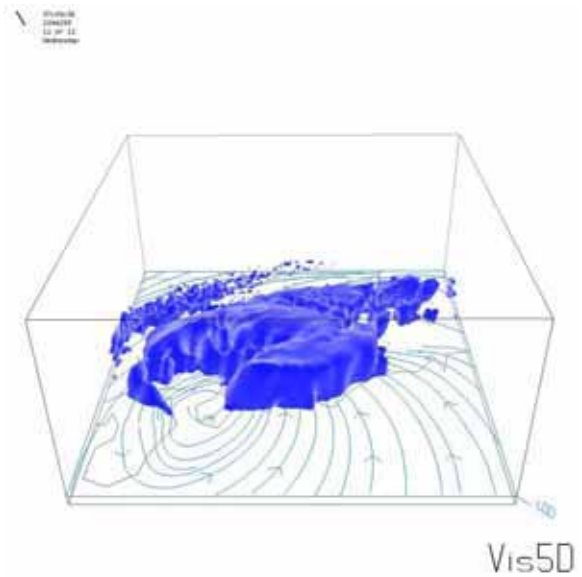

Fig.13 Bird eye view of simulation with MM5

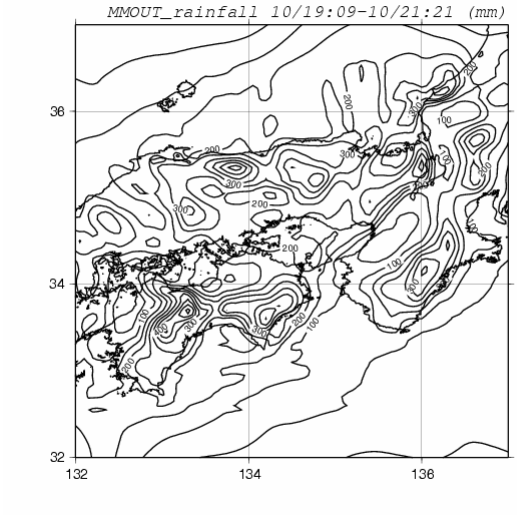

Fig.14 Accumulated Precipitation

3.2 Land surface – Atmosphere interaction

It is important to investigate the Asian monsoon and its variability to understand the abnormal weather in summer. In order to know the energy flux from the land surface to the atmosphere, which largely controls the

Asian monsoon, a satellite data based methodology has been developed and is applied to the Tibetan Plateau. This is called the Surface Energy Balance System (SEBS) and is originally developed for NOAA/AVHRR data. We modified this system to use GMS-5/VISSR data and other supplemental meteorological data. Surface temperatures obtained from the GMS data were put into the SEBS to estimate the hourly regional distribution of the surface heat fluxes such as the net-radiation, soil heat flux and the sensible heat flux. The last component, the latent heat flux, is calculated as the residual of the three components using surface energy balance equation. The estimated fluxes are verified by using corresponding field observations measured at Amdo with a sonic anemometer-thermometer corrected by using the eddy correlation methodology. The diurnal cycle of estimated fluxes agreed with the field measurements. For example, the diurnal range of the estimated sensible heat flux decreases from June to August (Figure 15). This reflects the change of dry to wet surface characteristics due to frequent precipitation during the summer monsoon. Over the Tibetan Plateau, the diurnal range of the surface temperature is as large as the annual range, so that the resultant sensible heat flux has a large diurnal variation. Thus, the hourly estimation based on the GMS data may contribute to a better understanding of the land surface-atmosphere interaction in this critical area.

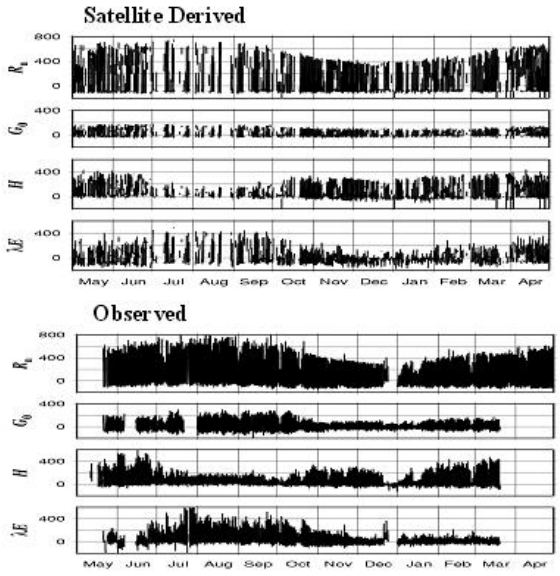

Fig.15 Comparison of satellite derived and measured surface fluxes at Amdo, Tibet. Rn is the net radiation, G0 the soil heat flux, H the sensible heat flux and λE the latent heat flux.

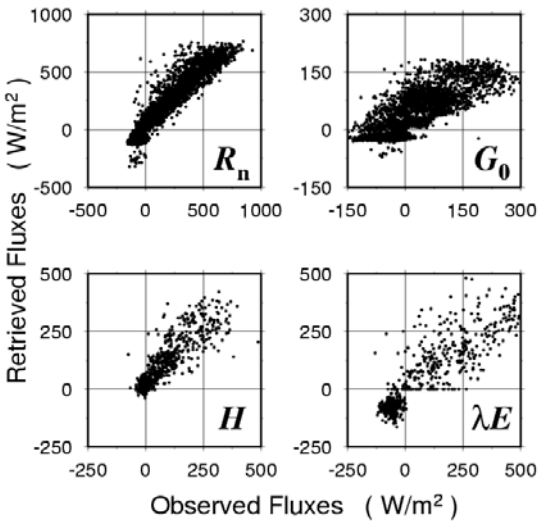

Fig.16 Scatter diagram of fluxes

References

Andrews, D. G., J. R. Holton, and C. B. Leovy, 1987: Middle Atmosphere Dynamics. 489 pp., Academic Press, Orlando.

Baldwin, M. P., and T. J. Dunkerton, 1999: Propagation of the Arctic Oscillation from the stratosphere to the troposphere. J. Geophys. Res., Vol. 104, 30937--30946.

Baldwin, M. P., and T. J. Dunkerton, 2001: Stratospheric harbingers of anomalous weather regimes. Science, Vol. 294, 581--584.

Japan Meteorological Agency, 2002: Outline of the operational numerical weather prediction at the Japan Meteorological Agency (JMA). Appendix to WMO Numerical Weather Prediction Progress Report, 157pp., JMA, Tokyo.

Matsuno, T. 1971: A dynamical model of stratospheric sudden warming. J. Atmos. Sci., 27, 871--883.

Mukougawa, H., and T. Hirooka, 2004: Predictability of stratospheric sudden warming: A case study for 1998/99 winter. Mon. Wea. Rev., 132, 1764--1776.

Naujokat, B., K. Kruger, K. Matthes, J. Hoffmann, M. Kunze, and K. Labitzke, 2002: The early major warming in December 2001--exceptional? Geophys. Res. Lett., 26, 29(21), 2023, doi:10.1029/2002GL015316.

Toth, Z., and E. Kalnay, 1993: Ensemble forecasting at NMC; the generation of perturbations. Bull. Am. Met. Soc., 74, 2317--2330.

異常気象とそれに伴う災害の実態把握と予測に関する研究

河井宏允・岩嶋樹也・植田洋匡・
石川裕彦・丸山敬・向川均
堀口光章・井口敬雄・荒木時彦

要旨

本報告は，異常気象を引き起こす原因の解明と，それによってもたらされる災害の実態について述べたもので３部からなっている。第１部では，　2001年12月に生じた成層圏突然昇温現象(Stratospheric Sudden Warming; SSW) の予測可能性を調べ，SSW は2週間以前から予測可能であり，SSW発生期には予測の初期値に対する鋭敏性が極めて大きくなることを見出した。第2部では，2004年9月7日から10日にかけて日本列島を縦断し，各地に多大な被害をもたらした台風0418号による強風被害について，世界遺産である宮島の厳島神社における現地被害調査を中心に，気象状況や被害状況等を解析した結果について述べている。

キーワード:異常気象，成層圏突然昇温，台風，強風被害，厳島神社，地形風、アジアモンスーン、衛星データ解析

異常気象とそれに伴う災害の実態把握と予測に関する研究

河井宏允・岩嶋樹也・植田洋匡・
石川裕彦・丸山敬・向川均
堀口光章・井口敬雄・荒木時彦

要旨

2004年，日本には1951年に台風の数が正式に数えられるようになって以来最多の10個の台風が上陸して，日本各地に多大な被害が生じた。本報告は，このような異常気象とそれを引き起こす要因を，メソスケールから地球規模に至る様々なスケールの現象の解析によって明らかにするとともに，それによってもたらされる災害の実態について述べたもので３部からなっている。

第１部では，近年，対流圏の予測可能性にも大きな影響を及ぼしていると指摘されている，北半球冬季に成層圏極渦が弱くなる成層圏突然昇温現象(Stratospheric Sudden Warming; SSW)についてSSW自体の発生要因や予測可能性を調査した。ここでは，気象庁一ヶ月アンサンブル予報結果を用いて，2001年12月に生じた波数1型の SSWの予測可能性やその前駆現象について解析を行った．その結果，このSSWは少なくとも2週間以前より予測可能であり，その発生期にはSSW予測の初期値に対する鋭敏性が極めて大きくなることが示された．またSSWの前駆現象として，対流圏上層での帯状風偏差が重要であり，北緯80(60)度付近で帯状風が強まる(弱まる)と，その後，成層圏極域で昇温しやすいことが示された．これは，このような帯状風偏差に伴い，対流圏上層での波の屈折率が変化し，SSWを引き起した波数1の惑星規模波の伝播方向をより極側に偏向させるためと考えられる．また，SSW発生期においてアンサンブルメンバー間の拡がりが最も大きくなる帯状風の偏差パターンは，SSWの前駆現象と考えられる帯状風の偏差パターンと一致していた．この両者のパターンが一致したため，SSW予測の初期値に対する鋭敏性が大きくなったと考えられる。

第２部では，2004年9月7日に広島県の厳島神社を襲った台風18号による被害について，現地調査を行い，厳島神社および周辺の被害や強風に関する各種データを集めた．それらの資料をもとに，当時の気象状況および被害の実態について明らかにした．厳島神社では本社拝殿，西回廊，客神社祓殿などの檜皮屋根のめくれ，能舞台の軒瓦の飛散などが強風による被害であった．また，回廊や平舞台，高舞台，火焼前，左楽房などが高潮と波によって被害を受けた．さらに，神社南側に延びる谷筋に沿って吹き降りる強風が被害状況や目撃証言などにより確認された．

第３部では，2004年の異常な台風の上陸の背景としての、2002年から2004年の広域海面温度の状況を明らかにするとともに，メソスケール気象モデル(PSU/NCAR MM5)による数値シミュレーションによって，台風時の気象状況を再現した。再現結果は観測結果と良く一致した。また，台風の発生など，アジアモンスーンの変動に大きな影響を与えているチベット高原に関して、GMS-5のデータを用いて、高原地表面温度の長期変化傾向を明らかにした。